Viscoelasticity of Epoxy Resin/Silica Hybrid Material Prepared via Sol–Gel Process: Considered in Terms of Morphology

Wakako Araki, Tadaharu Adachi

Department of Mechanical Sciences and Engineering, Tokyo Institute of Technology, 2-12-1 O-okayama, Meguro-ku, Tokyo 152-8552, Japan

Received 16 April 2007; accepted 25 June 2007
DOI 10.1002/app.27019
Published online 13 September 2007 in Wiley InterScience (www.interscience.wiley.com).

ABSTRACT: We investigated the relationship between the morphology and viscoelasticity of epoxy/silica hybrid materials manufactured via two different processes: simultaneous formation of epoxy and silica phases and sequential formation of silica phase in the prepared epoxy phase. The glass transition phenomena of the hybrid materials mostly depended on their silica structure. The particular structure did not affect T_g much, while the silica chain structure greatly raised T_g of the hybrid samples. The storage modulus E' depended on the volume fraction of the silica phase ζ, rather than the silica structure. In the glassy state, E' of the hybrid samples slightly decreased when compared with the neat epoxy samples. Lack of chemical reaction between the silica and the epoxy phases could be attributed to this decrease at which the silica structure could have worked as a flaw. In the rubbery state, E' greatly increased with increasing silica content ζ regardless of the silica structure, and this behavior well agreed with that predicted by the Davies model, because the physical interaction worked very well in the rubbery region. © 2007 Wiley Periodicals, Inc. J Appl Polym Sci 107: 253–261, 2008

Key words: viscoelasticity; organic/inorganic hybrid material; epoxy resins

INTRODUCTION

Organic/inorganic hybrid material has been of great interest in various fields and is expected to exhibit novel properties as it has both organic and inorganic phases blended on a molecular level.

The manufacturing processes of organic/inorganic hybrid materials have been investigated in recent years.[1–30] The process principles can mainly be classified as follows: simultaneous formation of organic and inorganic phases,[4,10,19,21,30] formation of the inorganic phase in the prepared organic phase,[4,19,21] and cooperation of the organic phase to the inorganic phase.[5,6] In addition, some modifications or functionalizations of organic polymers are also effective for controlling morphology and achieving a good adhesion between organic and inorganic phases. The first and second processes are generally effective for improving properties of organic materials by hybridization, and the third one is generally used to improve the properties of inorganic materials.

The most common process for incorporation of inorganic phase into organic phase is a sol–gel reaction by using metal alkoxides such as tetraethoxysilane, which produce inorganic phase through two reactions of hydrolysis and polycondensation. The sol–gel process has been applied to many organic polymers[7–30] such as poly(methyl methacrylate),[7–11] polyimide,[12–14] poly(ehyleneoxide),[15] phenolic resin,[16] and so on, to produce organic/inorganic hybrid materials. As for epoxy resin,[17–30] several researchers have worked on hybrid materials prepared via sol/gel process as well and reported great improvements in properties such as high thermal stability and high glass transition temperature.

Most of the researches on organic/inorganic hybrid materials were focused on starting materials and manufacturing processes for a good bonding between the both organic and inorganic phases and on morphologies, rather than mechanical properties.[16,23,24,29,30] For further application to engineering fields, mechanical properties such as viscoelasticity should be considered in more detail and a useful model is required to predict mechanical properties in terms of morphology of hybrid materials.

The purpose of this study is to clarify the relationship between the morphology and viscoelasticity of epoxy/silica hybrid materials manufactured via two different processes: simultaneous formation of epoxy

Correspondence to: W. Araki (araki@mech.titech.ac.jp).
Contract grant sponsors: Canon Foundation in Europe; Ogasawara Foundation.

Journal of Applied Polymer Science, Vol. 107, 253–261 (2008)

TABLE I
Prepared Samples

Sample name	TEOS : IP in volume	TEOS: D2000 in mass	Order of immersion (TEOS, IP, TSA, H_2O)	Silica content in weight	Silica content ϕ, in volume	Storage modulus E', GPa (at 183 K)	Storage modulus E', GPa (at 403 K)
Epo	–	–	–	0.000	0.000	4.80	0.003
Sim A1	45 : 55	33 : 67	–	0.097	0.059	3.04	0.033
Sim A2	45 : 55	50 : 50	–	0.178	0.108	4.02	0.091
Seq B1	10 : 90	–	Altogether	0.154 (0.188)	0.093 (0.114)	3.85 (2.27)	0.146 (0.035)
Seq B2	30 : 70	–	Altogether	0.052 (0.067)	0.032 (0.041)	3.64 (2.73)	0.048 (0.035)
Seq B3	50 : 50	–	Altogether	0.079 (0.087)	0.048 (0.053)	2.37 (3.13)	0.038 (0.036)
Seq C1	50 : 50	–	TEOS → IP, TSA, H_2O	0.182	0.110	6.68	0.106
Seq C2	50 : 50	–	TSA, H_2O → IP, TSA	0.077	0.047	3.49	0.083
Seq C3	50 : 50	–	IP → TEOS → TSA, H_2O	<0.001 (0.024)	<0.001 (0.015)	4.09 (4.29)	0.009 (0.005)

All samples were post-cured at 363 K for 24 h and at 403 K for 24 h. The values in parentheses for silica content and storage modulus show the ones of the aged samples.

and silica phase, and formation of silica phase in prepared epoxy phase.

EXPERIMENTAL PROCEDURES

Specimens

Diglycidyl ether of bisphenol A type epoxy resin (DGEBA) (DER331, Dow Chemical) and poly(oxypropylene)diamine (D2000) (Jeffamine D2000, Huntsman) were used as the organic components. For the sol–gel process to form an inorganic phase, tetraethoxysilane (TEOS) as an alkoxyl silane, *p*-toluensulfonic acid monohydrate (TSA) as a catalyst, diluent isopropyl alcohol (IP) as a solvent, and water (H_2O) were used. The molar ratio of TSA : TEOS and H_2O:TEOS were 2 : 100 and 3 : 1, respectively. The mixture ratio and the manufacturing processes of the hybrid samples in this study basically followed the references.[18,21,31]

For neat epoxy resin samples called Epo in this study, DGEBA and D2000 were blended with a stoichiometrical ratio, mixed thoroughly, degassed for 2 h, and cured at 363 K for 2 h and at 403 K for 2 h in a furnace.

For organic–inorganic hybrid samples, two different hybrid manufacturing processes were examined: one was a simultaneous hybrid manufacturing process and the other one was a sequential hybrid manufacturing process.

In the simultaneous hybrid manufacturing process, after TEOS was blended with TSA, IP, and water, this TEOS mixture was hydrolyzed at room temperature for 1 h. Then, DGEBA and D2000 were simultaneously blended in this TEOS solution with various mixture ratios of D2000 to TEOS, where D2000 worked as a curing agent and also a polymerization catalyst for TEOS. It was poured into a mould and kept at room temperature (293 K) over 21 days for gradual drying and polymerization. After that, the sample was placed in a furnace at 363 K for 12 h and at 403 K for 24 h to finish curing of the epoxy resin and also to complete the polycondensation process for hybridization. The samples prepared by this simultaneous process are called ''Sim A'' in this study.

In the sequential hybrid manufacturing process, the cured epoxy samples which were made by the same process as Epo were immersed in solutions in various orders, and the samples are called ''Seq B'' and ''Seq C.'' For preparation of Seq B, the epoxy sample was first immersed in a solution which consisted of TEOS, IP, TSA, and water at 333 K for less than 2 h. After it was taken out of the solution, it was gradually dried at room temperature for 3 days. For preparation of ''Seq C,'' the epoxy sample was first immersed in either TEOS or water with TSA at 313 K for 4 days, or IP at 333 K for 3 h and then in TEOS at 313 K for 1 day, followed by other immersions into the mixture of the others at 323 K for 1 day.

Table I shows the mixture ratio and summary of the hybrid manufacturing process for each hybrid sample. All samples of Epo, Sim A, Seq B, and Seq C were postcured at 363 K for 24 h and 403 K for 24 h.

Experiments

To evaluate the content of inorganic silica phase formed in the hybrid samples, the specimens were placed in a furnace (Carbolite, Eurotherm) at 1073 K for 4 h to pyrolyse the epoxy phase. The weights of each sample before and after the pyrolysis were measured.

The hybrid samples were observed with a transmission electron microscope (TEM) (JEM-2000FX-II and JEM-200CX, JEOL) to investigate microstructures. The samples for the TEM observation were prepared by an ultramicrotoming machine (Power Tome XL, RMC Product) with a cryoknife at 208 K and were cut into about 80 nm thick. Accelerating voltage between 100 and 180 kV was used accordingly.

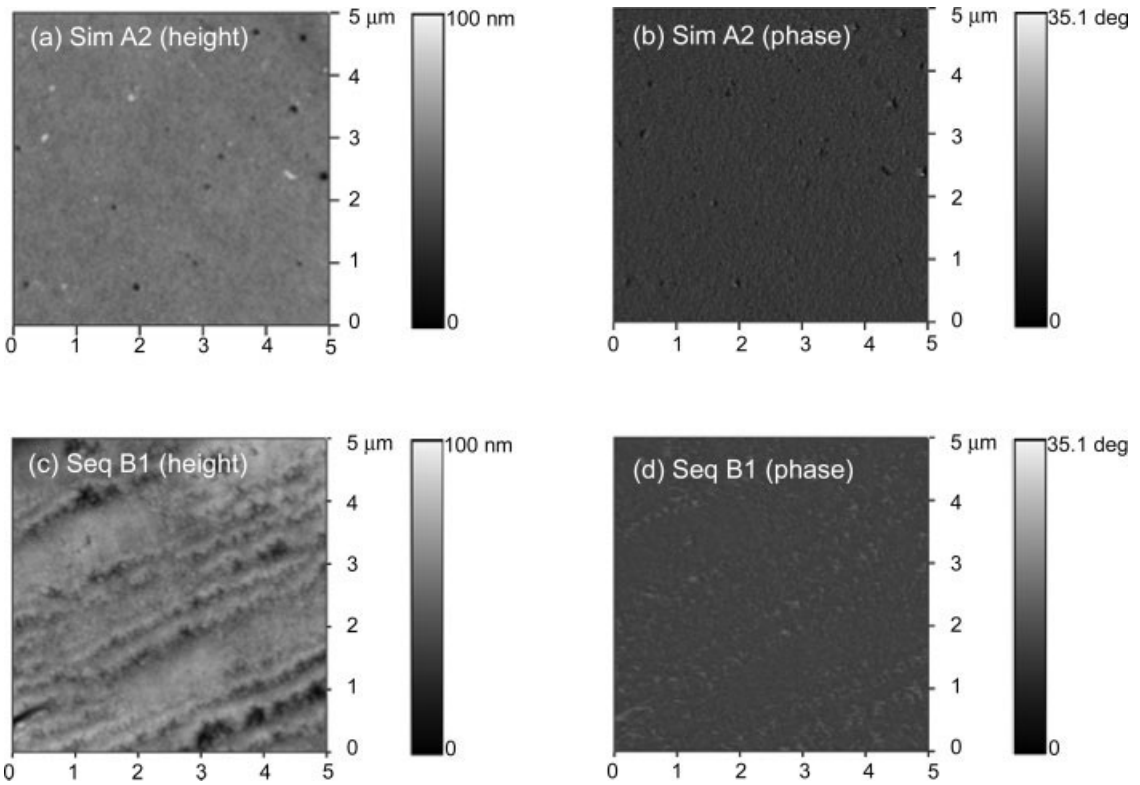

Figure 1 AFM height and phase images (scanning area is 5 × 5 μm^2).

The microtomed sections were also used for observation of the atomic force microscope observation (AFM) (SPM-9500J3, Shimazu). In the AFM observations, tapping mode was employed to obtain height images (topography) and phase images.

Raman spectroscopic analysis was performed with laser micro-Raman spectrometer (NRS-1000, JASCO). The hybrid samples were examined with a space resolution of 2 μm. A green laser with wavelength of 532.3 nm and a power of 100 mW was used, and the spectral slit was 50 μm wide. The exposure time was less than 120 s.

A dynamic tensile test (Tritec, Triton Technology) was carried out to measure dynamic moduli and glass transition temperature. Test frequency was 1 and 10 Hz, and the temperature range was from 173 K to 473 K with an increasing rate of 4 K/min.

To evaluate aging effects on the silica content and the viscoelasticity of the hybrid samples, the silica content measurement and the dynamic tensile test were performed again 4 months after manufacture. These samples were called ''aged'' samples in this study.

RESULTS AND DISCUSSION

Silica content

The silica content in each hybrid sample is summarized in Table I. The silica content in the total volume of each hybrid sample, ϕ, was calculated by using the relative density, 1.65×10^3 kg/m.[9,32] For Sim A, ϕ was high when the ratio of TEOS to D2000 was high. The produced silica in Sim A2 was 10.8 vol %. On the other hand, there was no correlation between the ratios of TEOS:IP and ϕ for Seq B and C. The reason for this could be that the TEOS solution itself started to polymerize during the immersion and also that the hybrid phase firstly was initially formed near the surface, which usually hindered the diffusion of the TEOS solution into the samples. Seq B1 with a low concentration of TEOS in the solution had a high ϕ of 9.3 vol %. Seq C1 which was first immersed in TEOS also had a high ϕ of 11.0 vol %, although it looked to have silica phase mostly near the surface. After aging, the silica content ϕ in the Seq B and C samples slightly increased.

Both the simultaneous and sequential hybrid manufacturing processes were able to create hybrid samples with approximately 10 vol % of the silica phase.

AFM and TEM observations

Since all samples were visually transparent, the size of the silica phase produced in all the hybrid samples was estimated to be smaller than optical wavelength, about 400 nm.

Figure 1 shows height and phase images of Sim A2 and Seq B1 obtained by AFM observation. Silica

particles ranging in size from 10 to 100 nm were dispersed in Sim A2 and no agglomeration was observed, while there was no particular feature in Seq B1 except for smearing marks in the height image because of the microtoming.

Figure 2(a) shows pictures of Sim A2 obtained by TEM observation. It was confirmed that the silica particles between 10 and 100 nm in size were dispersed in Sim A2, similar to what was shown in the AFM images. Although no silica particle was observed in Seq B or C, fine silica chains and their agglomeration were sparsely observed in them [Fig. 2(b,c)]. Thus, the fine silica chain structure could be formed in the Seq B and C samples.

It can be considered that, for Sim A, the sol–gel reaction proceeded simultaneously during the cross-linking reaction so that the silica particle and the epoxy phase were separately formed. On the other hand, the sol–gel reaction proceeded in the preexisted fine epoxy network which prevent formation of silica particles, so that the fine silica chain were formed in the epoxy phase.

Regarding the same hybrid system as the present study, Matejka et al.[21,31] conducted a fractal analysis based on their small angle X-ray scattering analysis and reported that the sample made by a sequential process had an ''open silica structure'' which had grown within an epoxy network with a size of less than 10 nm whereas a sample made with the simultaneous process consisted of ''small compact silica particles'' and a ''large loosen silica cluster'' with a size of 50–100 nm. The results of the AFM and TEM observation in our study agreed with theirs.

These AFM and TEM results showed that the silica particles with sizes between 10 and 100 nm were uniformly dispersed in the epoxy phase of the Sim A samples, which had a similar structure to that of the conventional particulate composite system. In the Seq B and C samples, fine silica chain structures on a scale of several hundreds nanometer or smaller could be formed in the epoxy phase.

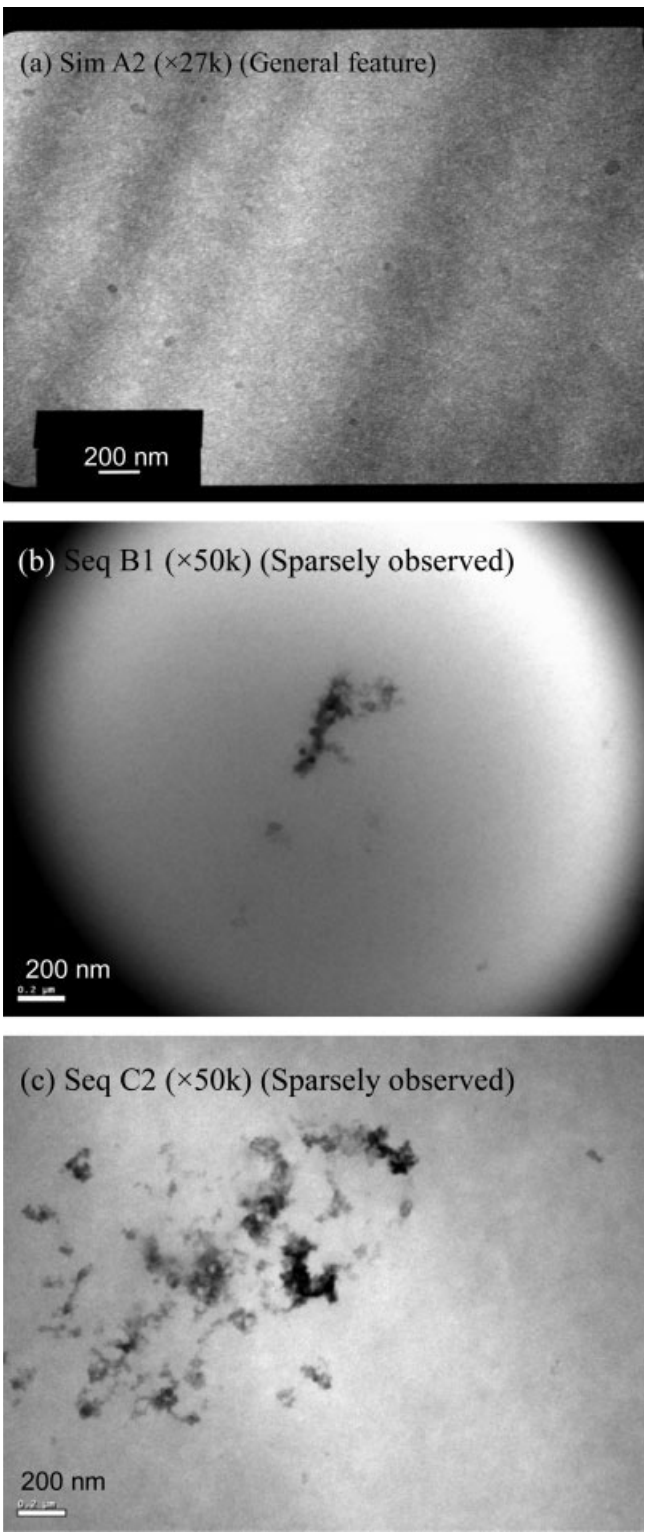

Figure 2 TEM pictures.

Raman spectroscopic analysis

Figure 3 shows the Raman spectra of Epo, Sim A2, Seq B1 and C1. The spectra between 3300 and 2500 cm^{-1} in Figure 3(a) were normalized by the peak intensity of the CH asymmetric vibration of bisphenol A at 2971 cm^{-1}, and those between 1700 and 300 cm^{-1} in Figure 3(b) by one of aromatic ring moiety at 639 cm^{-1}. Common spectra such as vibrations of the hydrocarbon groups between 3100 and 2800 cm^{-1}, and backbone vibration related to the bisphenol A between 950 and 800 cm^{-1} and the epoxy ring breathing between 1300 and 1200 cm^{-1} were seen in all samples. There was no particular peak between 4500 and 3500 cm^{-1} or between 2500 and 2000 cm^{-1}. The specific spectra and their proposed assignments are summarized in Table II.[33–46]

The Sim A samples had an identical spectrum to that of Epo, regardless of the hybridization. The same results of Raman analysis were reported for particulate composite systems.[47] This Raman spectro-

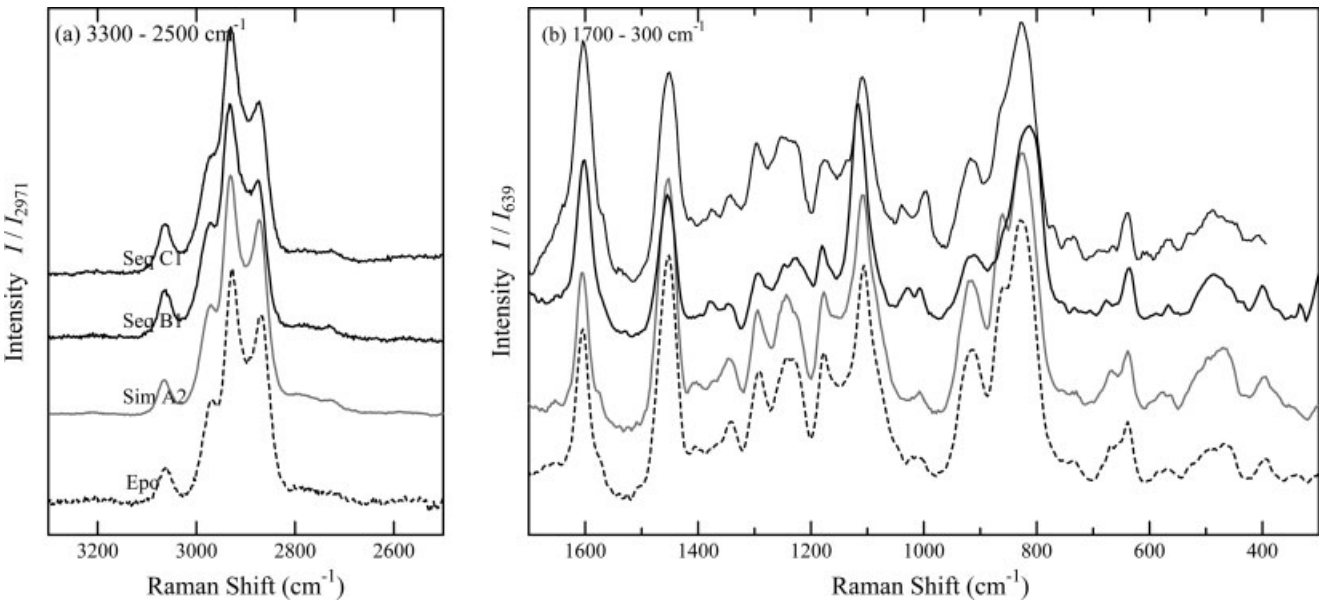

Figure 3 Raman spectra.

scopic analysis confirmed that the epoxy phase and the silica phase separately existed in Sim A and there was no chemical interaction between them.

Compared with Epo and Sim A, several differences were observed in the spectra of in Seq B and C. The intensities of all the spectra related to the epoxy ring, such as the peaks at 915 and 860 cm^{-1}, clearly decreased. The spectra of methyl groups including double methyl groups in bisphenol also decreased in intensity. The decreases of these peaks could be

TABLE II
Raman Spectra and Proposed Assignments

Raman shift (cm^{-1})	Proposed assignments for epoxy resin[33–39]	Proposed assignments for others[34,40–46]
2971	CH asymmetric stretch of BA	
2928	CH_2 asymmetric stretch	
2871	CH_3 asymmetric stretch or CH_2	
1604	CC aromatic ring buckle	
1455	CH_2 scissors or CC aromatic ring and CH_3 asym	
1344	Epoxy ring breathing vibration	
1291	CH_2 twist or/and CO stretch	
1244	Epoxy ring	
1228	Aromatic ether stretch	
1180		Si—O—Si asymmetric bond stretch (LO)
1177	Gem-dimethyl deformation of BA	
1116	Para-disubstituted phenyl group of BA	
1106	(CH in-plane)	
1030		Si—O—Si asymmetric bond stretch (TO)
1008	CC aromatic ring breathing	
980		Si—OH symmetric stretch
915	Epoxy ring	
860	Epoxy ring	
830	Para-disubstituted phenyl group of BA (CH out-of-plane)	
800		Si—O—Si bond stretch (SiO_2)
639	Aromatic ring moiety	
610		3-fold rings of SiO_2
540–460	CCC skeletal	
480		4-fold rings of SiO_2
430		Si—O—Si bond stretch (SiO_2)

attributed to physical interactions between the silica and the epoxy resin, not chemical reactions, because any peak of covalent reactions between organic and inorganic phases such as Si—O—C or Si—C which was supposed to be appeared around 900–1200 cm^{-1} was not observed.[34,48] Moreover, the spectrum of C—C—C backbone around 500 cm^{-1} deformed and also had a peak in higher Raman shift, which probably demonstrated the influence by amorphous silica spectra. In addition, the new peak appearing at 1030 cm^{-1} was considered to be the contribution of Si—O—Si asymmetric stretching, which could be related with a silica chain structure.[34,45,46] The effect of hybridization in the spectra of hydrogen bonds which was observed by FT-Infrared spectroscopy in another studies[24,48] is generally difficult to evaluate with the Raman spectroscopy.

The Raman spectroscopic analysis showed that Sim A had a structure in which the epoxy phase and the silica phase were completely separated without any interactions whereas Seq B and C had amorphous silica chains which physically interacted with the epoxy resin. Covalent bonds were not formed in either the simultaneous or the sequential hybrid manufacturing processes of this study.

Viscoelasticity

Figure 4 shows measured dynamic storage moduli, E', and mechanical losses, tan δ, of Epo, Sim A2, Seq B1, and Seq C1. In the glassy region below 200 K, E' of all the samples were several GPa and no clear effect of the hybridization was observed. In the rubbery region above 350 K, E's of the hybrid samples were above 10^{-1} GPa, which was much higher than that of Epo, about 10^{-3} GPa.

Also, the samples all had a large decrease in E' and a peak in tan δ around 240 K, because of the glass transition of the epoxy phase (GT1). In addition, another transition in E' and tan δ only for the Seq B and C at higher temperature [Fig. 4 (GT2)]. This transition was possibly caused by the relaxation phenomenon of the hybrid phase, where the silica chains physically interacted with the epoxy resin as discussed in AFM and TEM Observations and Raman Spectroscopic Analysis. Seq B and C seemed to have the same viscoelastic features regardless of the immersion order.

Considering their appearance described in Silica Content, these two transition phenomena illustrated that Seq B and C consisted of surface layers of hybrid phase and a middle layer of epoxy phase, whereas Sim A had a homogeneous hybrid structure. Both epoxy and hybrid phases in Seq B and C were in the glassy state below the temperature for GT1. Between GT1 and GT2, the hybrid phase was glassy so that a high modulus was maintained

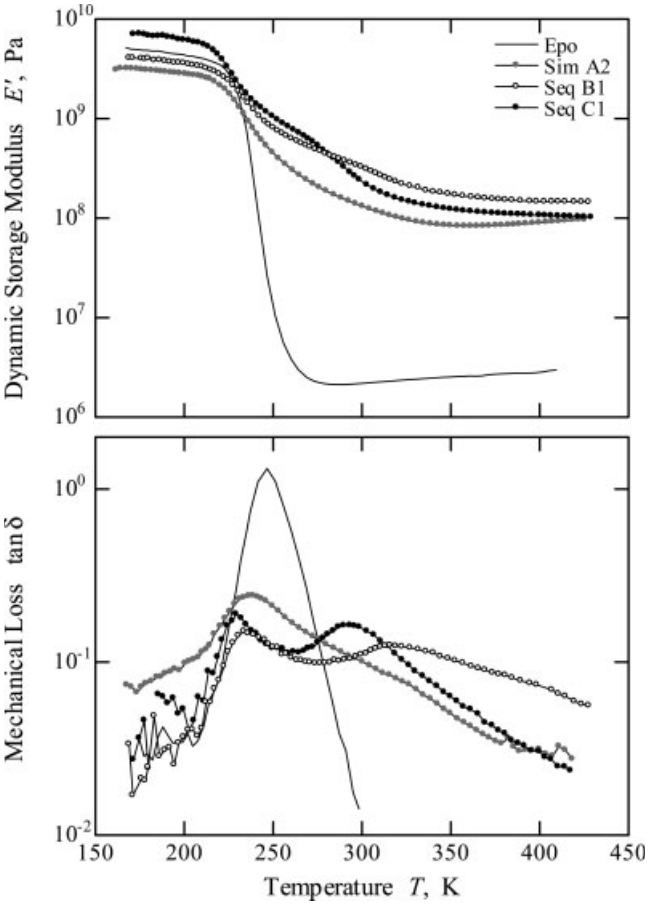

Figure 4 Dynamic storage modulus and mechanical loss (measurement frequency is 1 Hz). (–), Epo; (●), SimA2; (○) SeqB1; (◉), SeqC1.

whereas the epoxy phase was rubbery. Above the temperature for GT2, both phases were rubbery.

The measured values of E' at 183 K in the glassy region and at 403 K in the rubbery region are shown in Table II. There was no clear effect of aging on it.

DISCUSSION

For further discussion of the viscoelasticy, Seq B and C were considered as a layered material consisting of two surface layers of hybrid phase and one middle layer of epoxy phase as described earlier. The volume fraction of the hybrid phase (i.e. relative layer thickness of the hybrid phase) in each sample, ξ, and the modulus of the hybrid phase, E'_{hyb}, were briefly evaluated from a parallel model given by eq. (1),

$$E' = (1 - \xi)\, E'_{epo} + \xi\, E'_{hyb} \quad (1)$$

where E' is the measured storage modulus of each sample. E'_{epo} is the storage modulus of the epoxy phase, which is identical to that of Epo. To derive ξ and E'_{hyb} in the glassy and rubbery state, eq. (1) was

TABLE III
Silica Content and Dynamic Storage Modulus of Hybrid Phase of Seq B and C

Sample name	Hybrid phase ξ, in volume	Silica content in hybrid phase ζ, in volume	Storage modulus E'_{hyb}, GPa (at 183 K)	Storage modulus E'_{hyb}, GPa (at 403 K)
Seq B1	0.313 (0.687)	0.298 (0.167)	1.74 (1.12)	0.461 (0.050)
Seq B2	0.299 (0.490)	0.105 (0.083)	0.925 (0.578)	0.152 (0.068)
Seq B3	0.554 (0.425)	0.087 (0.124)	0.403 (0.877)	0.050 (0.081)
Seq C1	–	–	–	–
Seq C2	0.446	0.105	1.87	0.183
Seq C3	0.275 (0.145)	−(0.102)	−(1.25)	−(0.020)

The values in parentheses show the results of the aged samples.

employed at three different temperatures; at 183 K where both E'_{epo} and E'_{hyb} are of the glassy state, at about 260 K where E'_{epo} is of the rubbery state but E'_{hyb} is of the glassy state, and at 403 K where both are of rubbery state. The silica content in the hybrid phase, ζ, was evaluated from ξ by using

$$\zeta = \phi/\xi \tag{2}$$

ζ was 0 for Epo and ξ was 1 for Sim A.

ξ and ζ for Seq B and C are summarized in Table III. The modulus of the hybrid phase E'_{hyb} and the silica content in the hybrid phase ζ are used in the following discussion, instead of the measured modulus E' and the silica content in sample ϕ. Seq C1 was ruled out from this consideration as it had an additional glassy skin on the surface, which made its modulus higher than the other samples. Seq C3 as prepared was also excluded because ϕ was too small to measure experimentally (Table III).

The relationship between the silica content in the hybrid phase ζ and the glass transition temperature, T_g, is shown in Figure 5, where the peak temperature of tan δ measured at 1 Hz was defined as T_g. As above-mentioned, GT1 was the relaxation phenomenon of the epoxy resin itself, so that T_g for GT1 was approximately constant (about 240 K), regardless of either the hybrid manufacturing process or ζ. As for GT2, which was attributed to the relaxation of the hybrid phase of Seq B and C, T_g for GT2 was generally higher, at most 100 K higher, than the one for GT1.

Figure 6 shows the relationship between ζ and E' with conventional theoretical predictions for polymer composites and polymer blends: Voight, Reuss, Kerner, and Davies models (see Appendix). In the glassy region (183 K) shown in Figure 6(a), the val-

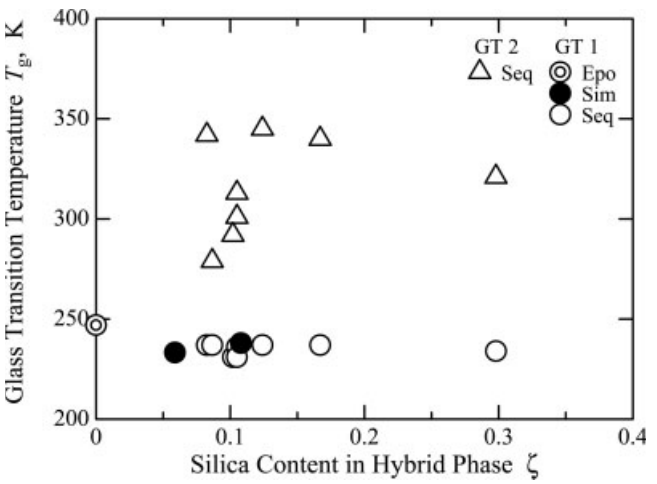

Figure 5 Glass transition temperature and silica content in hybrid phase. GT1: (◎), Epo; (●), SimA; (○), SeqB&C; GT2: (△), SeqB&C.

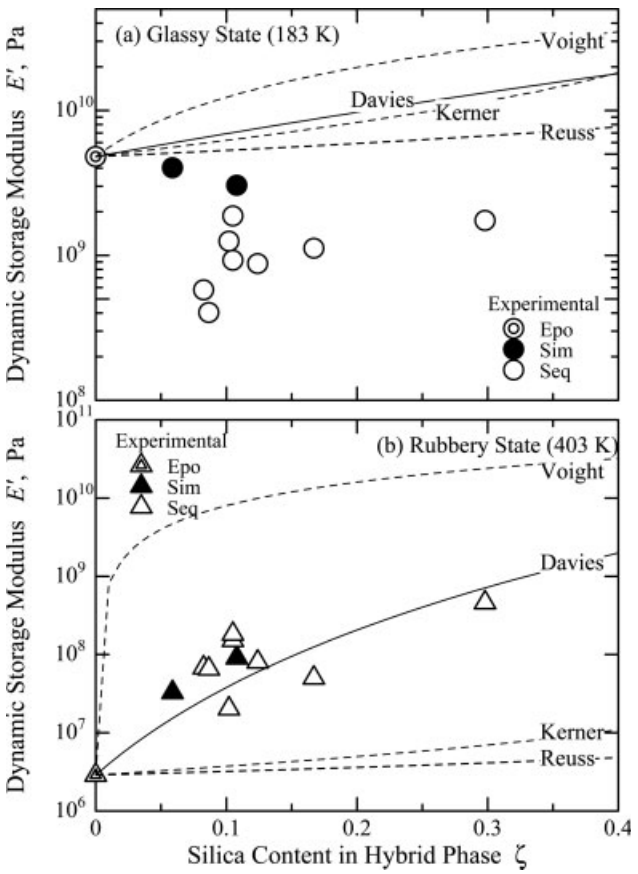

Figure 6 Dynamic storage modulus and silica content in hybrid phase with theoretical predictions. Experimental results: (◎), Epo; (●), SimA; (○), SeqB&C.

ues of E'_{hyb} were a little smaller than Epo. A slight decrease in E'_{hyb} for high ζ obviously disagreed with all of the theoretical models. On the other hand, E'_{hyb} in the rubbery region (403 K) increased with ζ as shown in Figure 6(b). E'_{hyb} with $\zeta = 0.3$ reached at maximum 10^2 times that of Epo, where E'_{hyb} in the rubbery state was very close to the one in the glassy state. The experimental results also agreed with the Davies model, which gives predictive fits to the experimental modulus of cocontinuous phases such as polymer blends, and they were way above the prediction of the Kerner model, which is often used to predict modulus of particulate composites.

Many studies[17,21,23–25,28,29,31] on organic/inorganic hybrid materials reported great increases in T_g (even disappearance of T_g), hardness, adhesiveness, and strength, and also modulus in the rubbery region. The results obtained in this study concerning T_g and E'_{hyb} in the rubbery region agreed with the results of those studies. The increase in T_g of the hybrid phase only for Seq B and C (Fig. 5) indicated that T_g depended on the hybrid process, i.e. the silica structure, not the silica content ζ. The comparison in Figure 6(b) proved that the Davies model is useful to predict E'_{hyb} in the rubbery region in terms of the silica content ζ, regardless of the silica structure. This could be because there was a strong physical interaction between the silica and the epoxy phase, which depended only on the silica content ζ. Moreover, the experimental and theoretical results indicated that when the silica content ζ is high, E'_{hyb} in rubbery state was close to, possibly rather higher than, that in the glassy state, which might lead to T_g-less materials that were reported in several papers.[24,28]

On the other hand, although several studies on organic/inorganic materials experimentally demonstrated no increases or small decreases in modulus in the glassy region, no clear explanation has been given before. As for nanoparticulate filled composite systems, despite that many researchers reported improvements in the mechanical properties, several researchers experimentally found that there was no improvement, rather a slight deterioration, in mechanical properties for the case that no strong chemical bonding was made between inclusions and matrix polymers.[49,50] It can be considered that the decrease in E'_{hyb} in the glassy state observed in this study can be attributed to the same reasons since no chemical reaction between the silica phase and the epoxy phase was confirmed by the Raman analysis.

CONCLUSION

In this study, epoxy resin/silica hybrid materials were prepared with two different hybrid manufacturing processes: the simultaneous formation of the epoxy and the silica phases, and the sequential formation of the silica phase in the prepared epoxy phase.

The observation with AFM, TEM, and Raman spectroscopic analysis confirmed the difference in microstructure depending on the hybrid process. In samples manufactured via a simultaneous process, the silica particles with sizes between 10 and 100 nm dispersed without agglomerating in the epoxy phase, in where the silica particle and the epoxy resin individually existed as in a conventional particulate composite. As for samples prepared by a sequential process, amorphous silica chain structures with a scale of a few nanometer or smaller were probably formed in the epoxy phase, in which the silica chain physically affected the epoxy resin.

The DMTA results demonstrated that the glass transition phenomena of the hybrid materials mostly depend on its silica structure in it. The particular structure did not affect T_g much, whereas the silica chain structure greatly raised T_g of the hybrid samples. The storage modulus E' depended on the volume fraction of the silica phase ζ, rather than the silica structure. In the glassy state, E' of the hybrid samples slightly decreased when compared with the neat epoxy samples. Lack of chemical reaction between the silica and the epoxy phases could be attributed to this decrease for which the silica structure could have worked as a flaw. In the rubbery state, E' greatly increased with increasing the silica content ζ regardless of the silica structure, and this behavior agreed with that of the Davies model, because the physical interaction worked very well in the rubbery region.

We would like to extend our gratitude to all the persons in the Mechanics of Materials research group of the Department of Mechanical Engineering, Imperial College London, especially Prof. Kinloch, for their kind help.

APPENDIX: THEORETICAL MODELS

Various models have been proposed to predict modulus of composite systems. The Voight model[51] gives an upper bound, E_U,

$$E(= E_U) = (1 - \zeta)E_1 + \zeta E_2 \quad \text{(A1)}$$

where E, E_1, and E_2 are modulus of composite, phase 1 (matrix phase) and phase 2 (minor phase). ζ is a content of phase 2.

On the other hand, the Reuss model[51] is known to give a lower bound, E_L.

$$E(= E_L) = (1 - \zeta)/E_1 + \zeta/E_2 \quad \text{(A2)}$$

Many researchers developed combined models from the parallel and the series ones.

Another important model for particulate composite systems is the Kerner model,[52] which allow for perfect adhesion between matrix and particles,

$$E = E_1(1 - AB\zeta)/(E_1 - B\Phi\zeta), \quad \text{(A3)}$$

where

$$A = (7 - 5\,\zeta)/(8 - 10\zeta)$$
$$B = (E_2/E_1 - 1)/(E_2/E_1 - A)$$
$$\Phi = 1 + \zeta(1 - \zeta_{max})/\zeta_{max}.$$

ζ_{max} is maximum packing ratio. It was assumed to be 0.6 in this study.

Davies model,[53] which assumes the blend to be macroscopically homogeneous and isotropic, is the most applicable to the experimental result of the cocontinuous structure without any details being specified,

$$E^{1/5} = (1 - \zeta)\,{E_1}^{1/5} + \zeta_2\,{E_2}^{1/5} \quad \text{(A4)}$$

In this study, the silica content of the hybrid phase ζ was considered for these theoretical equations. The moduli of the epoxy resin (Epo) at 183 K and 403 K were used as E_1 for predictions of the glassy and rubbery states, respectively. For E_2, the modulus of the silica (80 GPa) was used.

References

1. Klein, L. C. Sol–Gel Optics: Processing and Applications; Kluwer Academic Publishers: Dordrecht, 1994.
2. Coltrain, B. K.; Sanchez, C.; Schaefer, D. W.; Wilkes, G. L. Better Ceramics Through Chemistry VII: Organic/Inorganic Hybrid Materials; Materials Research Society: Pittsburgh, 1996.
3. Chujo, Y.; Saegusa, T. Adv Polym Sci 1992, 100, 11.
4. Bauer, B. J.; Liu, D. W.; Jackson, C. L.; Barnes, J. D. Polym Adv Technol 1996, 7, 333.
5. Haruvy, Y.; Webber, S. E. Chem Mater 1991, 3, 501.
6. Jang, J.; Park, H. J Appl Polym Sci 2002, 83, 1817.
7. Wei, Y.; Yang, D. C.; Bhakthavatchalam, R. Mater Lett 1992, 3, 261.
8. Silveira, K. F.; Yoshida, I. V. P.; Nunes, S. P. Polymer 1994, 36, 1425.
9. Tamaki, R.; Chujo, Y. J Mater Chem 1998, 8, 1113.
10. Yeh, J. M.; Weng, C. J.; Huang, K. Y.; Huang, H. Y.; Yu, Y. H.; Yin, C. H. J Appl Polym Sci 2004, 83, 94, 400.
11. Landry, C. J. T.; Coltrain, B. K.; Wesson, J. A.; Zumbulyadis, N.; Lippert, J. L. Polymer 1992, 33, 1496.
12. Nandi, M.; Conklin, J. A.; Salvati, L.; Sen, A. Chem Mater 1990, 2, 772.
13. Morikawa, A.; Iyoku, Y.; Kakimoto, M.; Imai, Y. Polym J 1992, 24, 107.
14. Ruan, S.; Lannutti, J. J.; Prybyla, S.; Seghi, R. R. J Mater Res 2001, 16, 1975.
15. Ravaine, D.; Seminel, A.; Charbouillot, Y.; Vincens, M. J Non-Cryst Solids 1986, 82, 210.
16. Haraguchi, K.; Usami, Y.; Ono, Y. J Mater Sci 1998, 33, 3337.
17. Mauer, B. J.; Liu, D. W.; Jackson, C. L.; Barnes, J. D. Polym Adv Technol 1995, 7, 333.
18. Matějka, L.; Dušek, K.; Pleštil, J.; Kříž, J.; Lednický, F. Polymer 1998, 40, 171.
19. Matějka, L.; Pleštil, J.; Dušek, K. J Non-Cryst Solids 1998, 226, 114.
20. Mascia, L.; Tang, T. J Mater Chem 1998, 8, 2417.
21. Matějka, L.; Dukh, O.; Kolařík, J. Polymer 2000, 41, 1449.
22. Mauri, A. N.; Riccardi, C. C.; Williams, R. J. J. Macromol Symp 2000, 151, 331.
23. Ochi, M.; Takahashi, R.; Terauchi, A. Polymer 2001, 42, 5151.
24. Ochi, M.; Takahashi, R. J Polym Sci Part B: Polym Phys 2001, 39, 1071.
25. Matsumura, T.; Ochi, M.; Nagata, K. J Appl Polym Sci 2003, 90, 1980.
26. Weng, W. H.; Chen, H.; Tsai, S. P.; Wu, J. C. J Appl Polym Sci 2004, 91, 532.
27. Macan, J.; Ivanković, H.; Ivanković, M.; Mencer, H. J. Thermochimica Acta 2004, 414, 219.
28. Fujiwara, M.; Kojima, K.; Tanaka, Y.; Nomura, R. J Mater Chem 2004, 14, 1995.
29. Lu, S. R.; Hongyu, J.; Zhang, H. L.; Wang, X. Y. J Mater Sci 2005, 40, 2815.
30. Yano, S.; Ito, T.; Shinoda, K.; Ikake, H.; Hagiwara, T.; Sawaguchi, T.; Kurita, K.; Seno, M. Polym Int 2005, 54, 354.
31. Matějka, L.; Dukh, O. Macromol Symp 2001, 171, 181.
32. Murtagh, M. J.; Graham, E. K.; Pantano, C. G. J Am Ceram Soc 1986, 69, 775.
33. Dollish, F. R.; Fateley, W. G.; Bentley, F. F. Characteristic Raman Frequencies of Organic Compounds; Wiley: New York, 1974.
34. Colthup, N. B.; Daly, L. H.; Wiberley, S. E. Introduction to Infrared and Raman Spectroscopy; Academic Press: New York, 1975.
35. Mertzel, E.; Koenig, J. L. Adv Polym Sci 1986, 78, 73.
36. Chike, K. E.; Myrick, M. L.; Lyon, R. E.; Angel, S. M. Appl Spectrosc 1993, 47, 1631.
37. Lyon, R. E.; Chike, K. E.; Angel, S. M. J Appl Polym Sci 1994, 53, 1805.
38. Younes, M.; Wartewig, S.; Lellinger, D.; Strehmel, B.; Strehemel, V. Polymer 1994, 35, 5269.
39. Tait, J. K. F.; Edwards, H. G. M.; Farwell, D. W.; Yarwood, J. Spectrochim Acta 1995, A51, 2101.
40. Bertoluzza, A.; Fagnano, C.; Morelli, M. A. J Non-Cryst Solids 1982, 48, 117.
41. Pancrazi, F.; Phalippou, J.; Sorrentino, F.; Zarzycki, J. J Non-Cryst Solids 1984, 63, 81.
42. Brinker, C. J.; Tallant, D. R.; Roth, E. P.; Ashley, C. S. J Non-Cryst Solids 1986, 82, 117.
43. Matsui, K.; Satoh, H.; Kyoto, M. J Ceram Soc J Jpn 1998, 106, 528.
44. González, P.; Serra, J.; Liste, S.; Chiussi, S.; León, B.; Pérez-Amor, M. J Non-Cryst Solids 2003, 320, 92.
45. Oh, T. Jpn J Appl Phys 2005, 44, 4103.
46. Lin, Y.; Tsui, T. Y.; Vlassak, J. J. J Electrochem Soc 2006, 153, F144.
47. Araki, W.; Adachi, T.; Yamaji, A. JSME Inter J 2003, 46, 2266.
48. Frings, S. Organic-Inorganic Hybrid Coatings: Based on Polyester Resins and In Situ Formed Silica; Technische Universiteit Eindhoven: Eindhoven, 1999.
49. Ciprari, D. L. Mechanical Characterization of Polymer Nanocomposites and the Role of Interface; Georgia Institute of Technology: Georgia, 2004.
50. Jinguo, Z.; Wilkie, C. A. Polymer 2006, 47, 5736.
51. Nielsen, L. E. Mechanical Properties of Polymers and Composites; M Dekker: New York, 1974.
52. Kerner, E. H. Proc Phys Soc 1956, 69, 808.
53. Davies, W. E. A. J Phys D Appl Phys 1974, 4, 1325.